Characterization of immunoreactivity with whole-slide imaging and digital analysis in high-grade serous ovarian cancer

Tiina Jäntti[1]* [ID], Satu Luhtala[2]*, Johanna Mäenpää[1,3] and Synnöve Staff[1,3,4]

Abstract

Ovarian cancer is the most lethal of gynecological cancers with 5-year survival rate of ca. 45%. The most common histologic subtype is high-grade serous carcinoma, which typically is presented with advanced stage and development of chemoresistance. Therefore, new treatment options, including immunotherapies, are needed. Understanding the features of the immune cell populations in the tumor microenvironment is essential for developing personalized treatments and finding predictive biomarkers. Digital image analysis may enhance the accuracy and reliability of immune cell infiltration assessment in the tumor microenvironment. The aim of this study was to characterize tumor microenvironment in a retrospective cohort of high-grade serous carcinoma samples with whole-slide imaging and digital image analysis. Formalin-fixed paraffin-embedded high-grade serous carcinoma tumor tissue samples (n = 67) were analyzed for six immunohistochemical stainings: CD4, CD8, FoxP3, granzyme B, CD68, and CD163. The stained sample slides were scanned into a digital format and assessed using QuPath 0.1.2 and ImageJ software. Staining patterns were associated with clinicopathological data. The higher numbers of intraepithelial CD8+, CD163+, and granzyme B+ immune cells were associated with survival benefit when analyzed individually, while high levels of both CD8+ and granzyme B+ tumor-infiltrating lymphocytes were an independent prognostic factor in the Cox multivariate regression analysis (median progression-free survival; hazard ratio = 0.287, p = 0.002). Specimens taken after administration of neoadjuvant chemotherapy presented with lower FoxP3+ tumor-infiltrating lymphocyte density (Fisher's exact test, p = 0.013). However, none of the studied immunomarkers was associated with overall survival or clinical factors. Tumors having high amount of both intraepithelial CD8+ and granzyme B+ tumor-infiltrating lymphocytes showed better progression-free survival, possibly reflecting an activated immune state in the tumor microenvironment. The combined positivity of CD8 and granzyme B warrants further investigation with respect to predicting response to immune therapy. Neoadjuvant chemotherapy may have an effect on the tumor microenvironment and therefore on the response to immuno-oncologic or chemotherapy treatments.

[1]Faculty of Medicine and Health Technology, University of Tampere, Tampere, Finland
[2]Department of Pathology, Seinäjoki Central Hospital, Seinäjoki, Finland
[3]Tays Cancer Centre, Tampere University Hospital, Tampere, Finland
[4]Department of Gynecology and Obstetrics, Tampere University Hospital, Tampere, Finland
*The first and the second authors contributed equally.

Corresponding author:
Tiina Jäntti, Faculty of Medicine and Health Technology, University of Tampere, Arvo Ylpön katu 34, 33520 Tampere, Pirkanmaa, Finland.
Email: tiina.jantti@tuni.fi

Introduction

Ovarian cancer (OC) is the third most common and the most lethal gynecological cancer.[1] High-grade serous carcinoma (HGSC) is the most common histological subtype, characterized by aggressive dissemination.[2,3] The standard treatment of OC is primary cytoreductive (debulking) surgery (PDS), followed by platinum-based combination chemotherapy with or without bevacizumab.[4–6] In some cases with advanced disease, neoadjuvant chemotherapy (NACT) and interval debulking surgery (IDS) may be considered.[4,7,8] The poor prognosis in OC (5-year survival ca. 45%) is caused by late diagnosis (67%–75% at FIGO III–IV) due to lack of specific symptoms and screening methods and by the development of chemoresistance over cumulative treatment lines.[2,4] Most of the patients respond to primary treatment.[4] However, nearly 80% of patients with advanced disease will relapse and recurrence is mostly incurable.[4] Despite the recent paradigm shift in frontline OC treatment with poly ADP ribose polymerase (PARP) inhibitors,[9–11] there is still urgent need for new OC treatment options, including immunotherapies. Immune cells and immunoregulatory molecules present in the tumor microenvironment (TME) are involved both in anti-tumor immune responses of the host and in immunosuppressive mechanisms promoting cancer progression.[12–14] Understanding the nature and characteristics of TME is essential for developing immuno-oncological treatment options and discovering predictive biomarkers for patient selection.[12–14]

Tumor-infiltrating lymphocytes (TILs) infiltrate to the tumor epithelium (intraepithelial, ieTILs) or locate at the peritumoral stroma (stromal, sTILs).[15] Intraepithelial CD3+ TILs (T cells) have been associated with improved patient outcome in OC.[16–21] When assessing the subsets of T cells, particularly CD8+ TILs (cytotoxic T-lymphocytes, Tc or CTL),[17–20,22–26] and, in some studies, CD4+ TILs (T helper, Th)[22] have been associated with favorable prognosis. Activated CTLs and natural killer (NK) cells eliminate cancer cells by secreting cytolytic enzymes, including granzyme B.[27]

FoxP3+ regulatory T cells (Tregs) may in turn suppress anti-tumor immunity.[15] The reports of impact of Tregs on prognosis of OC or other cancers have been contradictory.[18,19,24,28–30] Tumor-associated macrophages (TAMs) are further divided into M1 and M2 subtypes, of which M1 TAMs contribute to elimination of cancer cells, whereas anti-inflammatory M2 type is involved with tissue repair, angiogenesis and cancer progression.[31] There is no clear consensus on the role of M1 and M2 type of TAMs in OC, but according to available data, CD68+ (M1 and M2) TAM density may not act as prognostic factor.[19,21,32–34]

In addition, administration of NACT may alter the immune cell populations in TME. Although previously considered immunosuppressive, NACT has more recently been found to have anti-tumor immunity enhancing effects.[35] However, results considering the impact of NACT on the immune cells in OC TME and the prognostic significance of post-NACT TILs have been highly variable.[20,25,30,36,37]

Immune cell infiltration in OC has been studied extensively, yet results considering the prognostic significance of immune cells in the TME are highly variable.[15,18] Currently, there are no established cut-off values or analyzing methods for assessment of TILs, which may weaken the reproducibility of the studies. The use of whole-slide imaging (WSI) and digital image analysis (DIA) has been found to increase the reliability and accuracy of assessment of immune cells when compared to manual analysis and semi-quantitative scales.[38,39] Therefore, this study focusing on HGSC was set up to clarify, which immune cells or biomarkers present in TME are associated with clinical outcome. In this study, only intraepithelial immune infiltration was analyzed, as previous studies state that intraepithelial immune infiltration may have a stronger effect on prognosis than stromal infiltration. For optimal accuracy, WSI and DIA were used in the analyses.

Materials and methods

Patients and samples

The study was carried out at the Tampere University Hospital (TAUH) and the Faculty of Medicine and Health Technology, University of Tampere, Tampere, Finland. The study protocols have been approved by the Regional Ethics Committee of the Expert Responsibility area of Tampere University Hospital (identification codes: ETL-R09108 and ETL-R11137). All the study patients have provided a signed informed consent.

The present retrospective study cohort is consisted of tumor samples from two different cohorts of epithelial ovarian cancer (EOC) patients who had undergone PDS or IDS in TAUH during 2001–2009 and 2011–2013. Patients were recruited to the study when they were being treated with chemotherapy in either adjuvant or recurrent setting (older surgery cohort of 2001–2009) or when they have been scheduled for EOC surgery (surgery cohort of 2011–2013). The morphological and histological findings from the available and representative archival surgical tumor specimens were assessed by experienced pathologists at the Department of Pathology of TAUH. Only samples from patients with histologically verified high-grade OC were

included in the final study cohort, which consisted of 67 high-grade OC samples having sufficient tumor tissue content and technical quality for analyses.

Clinical, pathological, and follow-up data were collected from the patient records. As the patients were operated prior to 2014, the staging was adjusted to the FIGO 2014 staging classification. Surgical outcome was classified as following: R0 = no macroscopic residual tumor, R1 = residual tumor <1 cm, and R2 = residual tumor >1 cm. Median age at diagnosis was 63 years (range 38–78). Almost all patients (n = 64; 96%) had a verified HGSC histology. Most of the patients (n = 60; 90%) presented with an advanced stage disease (FIGO III/IV) with a median overall survival (OS) of 52 months (range 11–163) and progression-free survival (PFS) of 16 months (range 5–124). The main clinico-pathological characteristics of the study patients are summarized in Table 1.

Immunohistochemical stainings and interpretation

The HGSC tissue samples were formalin-fixed and paraffin-embedded (FFPE) prior to immunohistochemical (IHC) stainings. FFPE samples were cut into 3–4 µm thick sequential sections that were then baked, deparaffinized and pretreated by boiling them in Tris-EDTA buffer (pH 9) at +98°C for 15 min for epitope retrieval. IHC stainings were performed by indirect horseradish peroxidase (HRP)–based detection technique. Six IHC stainings were performed: CD4, CD8, FoxP3, granzyme B, CD68, and CD163. The antibodies, clones, and used dilutions are presented in Table 2. The tissue sections were counterstained with Mayer's hematoxylin (Oy FF-Chemicals Ab, Haukipudas, Finland) to give contrast for positive staining reaction visualized as brown diaminobenzidine (DAB) precipitate. Staining protocols were carried out with Autostainer 480 (Lab Vision, Fremont, CA, USA) automated immunostainer.

The stained sample slides were scanned into a digital format using the Hamamatsu NanoZoomer S60 Digital Slide Scanner. The digital whole-slide images (WSIs) were analyzed using QuPath 0.1.2 DIA software.[40] Three hot spot areas of 1 mm^2 tumor tissue were selected from each slide by visual observation. The hot spots were selected separately by an experienced cell biologist (S.L.) and the first author (T.J.). The criteria for selecting the hot spot areas were the presence of maximum extent of immune cell infiltration in tumor epithelium. As this study focuses on intraepithelial immune infiltration, areas with a wide extent of stromal tissue were excluded from the analyses. For CD4, CD8, FoxP3, and granzyme B stainings, the positively stained intraepithelial immune cells in each 1 mm^2 area were counted digitally using QuPath. In selected cases, the cell counts were assessed both digitally by QuPath and

Table 1. Patient characteristics.

	Total (n = 67)
Patient cohort 2001–2009; n (%)	32 (47.8)
Patient cohort 2011–2013; n (%)	35 (52.2)
Age at diagnosis (y); median (range)	63 (38–80)
Stage at diagnosis; n (%)	
I	1 (1.5)
IIA/IIB	6 (9.0)
IIIA/IIIB	3 (4.5)
IIIC	41 (61.2)
IVA/IVB	16 (23.9)
Grade; n (%)	
1–2	0 (0.0)
3	67 (100.0)
Histology; n (%)	
Serous	63 (94.0)
Transitional cell	1 (1.5)
Other or undefined epithelial	3 (4.5)
Ca 12-5 prior to treatment (kU/l); median (range)	719 (11–8909)
Ca 12-5 after treatment (kU/l); median (range)	16 (5–904)
BRCA status; n (%)	
Wild type	7 (10.4)
BRCA1	0 (0)
BRCA2	3 (4.5)
Not tested	57 (85.1)
Anti-inflammatory medication; n (%)	
Yes	4 (6.0)
No	63 (94.0)
Other cancers, n (%)	
Yes, breast	4 (6.0)
Yes, other than breast	4 (6.0)
No	59 (88.1)
Residual disease; n (%)	
R0	16 (23.9)
R1	12 (17.9)
R2	39 (58.2)
First-line chemotherapy; n (%)	
Paclitaxel-carboplatin	23 (34.3)
Paclitaxel-carboplatin-bevacizumab	11 (16.4)
Paclitaxel-carboplatin, switched to another platinum-based during first-line treatment	27 (40.3)
Other platinum-based	6 (9.0)
First-line chemotherapy cycles; median (range)	6 (4–18)
Neoadjuvant chemotherapy; n (%)	
Yes	15 (22.4)
No	52 (77.6)
Overall survival (m); median (range)	52 (11–163)
Progression-free survival (m); median (range)	16 (5–124)
Platinum-free interval (m); median (range)	10 (0–120)
Alive; n (%)	
Yes	14 (20.9)
No	53 (79.1)
Recurrence; n (%)	
Platinum sensitive (complete, 12 m) at first recurrence	22 (32.8)
Platinum sensitive (partial, 6–12 m) at first recurrence	16 (23.9)
Platinum resistant at first recurrence	21 (31.3)
No recurrence	8 (11.9)

BRCA: breast cancer gene.

Table 2. Antibodies used for immunohistochemical stainings.

Antibody	Detectable cells	Clone	Host species	Manufacturer	Dilution
FoxP3	Tregs	236A/E7	Mouse mAb	Abcam	1:100
Granzyme B	Activated lymphocytes and NK cells	BSR150	Rabbit mAb	Nordic Biosite	1:300
CD4	Th	BSR4	Rabbit mAb	Nordic Biosite	1:300
CD8	Tc (CTL)	BSR5	Rabbit mAb	Nordic Biosite	1:200
CD68	M1 and M2 macrophages	KP1	Mouse mAb	Zeta Corporation	1:1200
CD163	M2 macrophages	Ed-Hu1	Mouse mAb	Bio-Rad	1:700

NK: natural killer; CTL: cytotoxic T-lymphocyte; mAb: monoclonal antibody.

manually by counting the cells of the $1\,mm^2$ area in question. All manually revised cell counts were in line with the results obtained by digital analyses. For CD68 and CD163 stainings, the percentages of positively stained area/$1\,mm^2$ tumor tissue on the hot spot areas were analyzed. The hot spot areas were selected using QuPath as described before, and the percentages of positively stained areas on the hot spots were calculated using ImageJ.[41] The mean cell count (FoxP3, granzyme B, CD4, and CD8) or positively stained proportion (CD68 and CD163) of the three selected hot spots was calculated for each image. The above-mentioned analyses were performed separately by S.L. and T.J. The mean of the obtained results was used for statistical analyses. Any discrepancies between the analyses were discussed until a consensus was achieved. The proportions of tumor, stroma, and immune cells were assessed from the representative hematoxylin and eosin stained blocks using QuPath 0.2.1. These data are summarized in Supplementary Table 1. Examples of digital analyses are shown in Supplementary Figure 1.

Statistical analyses

Statistical analyses were performed using IBM SPSS Statistics 25.0 software. PFS was defined as time from diagnosis to the first recurrence. OS was defined as time from diagnosis to death. Data were censored to the last follow-up for patients who were alive and/or had no recurrence at the time of data collection.

Kolmogorov–Smirnov test and Shapiro–Wilk test were used for determining the normality of the variable distributions. Medians of cell densities or positively stained percentages/$1\,mm^2$ tumor tissue were compared between groups using Mann–Whitney *U*-test. Chi-square test and Fisher's exact test were used when comparing log-transformed cell densities or positively stained proportions as dichotomous variables. Kaplan–Meier method was used for analyzing cumulative survival, and differences in survival between groups were compared by log-rank test. A cut-off value for cell densities or positively stained percentages was set at the lowest 10th percentile. In addition, cut-offs at first,

Table 3. Sample topography.

	Total (n = 67)	
	n	%
Ovary	45	67.2
Fallopian tube	5	7.5
Adnexa (not otherwise specified)	10	14.9
Uterine serosa, tubal serosa	1	1.5
Omentum	2	3.0
Peritoneum	1	1.5
Sigmoid colon	1	1.5
Topography unknown	2	1.5

second, and third quartiles were tested. Hazard ratios (HRs) and 95% confidence intervals (CIs) were analyzed by the Cox proportional hazards regression model. Cell densities or positively stained proportions/ $1\,mm^2$ tumor tissue were log transformed when analyzed as continuous variables in regression models. Cell densities that showed a significant correlation with survival in univariate Cox regression analysis were entered to a multivariate analysis with known prognostic factors: size of residual tumor after surgery (R0 or R1/R2), NACT, and stage at diagnosis (FIGO I/II or III/IV). p-value $\leqslant 0.05$ was considered statistically significant.

Results

The final study cohort consisted of 67 high-grade OC samples. The sample topography is presented in Table 3. Most of the analyzed samples originated from the adnexa (89.6%). High individual variation in the densities of CD4+ (0–2416 cells/mm^2), CD8+ (1–4020 cells/mm^2) and granzyme B+ cells (3–3028 cells/mm) was observed. Median cell densities (CD4+, CD8+, FoxP3+ and granzyme B+) or median percentages of positively stained areas (CD68+ and CD163+) are summarized in Table 4, and examples of immunostainings are presented in Figure 1. A correlation between prolonged median PFS (17.00 vs 9.00 months for all
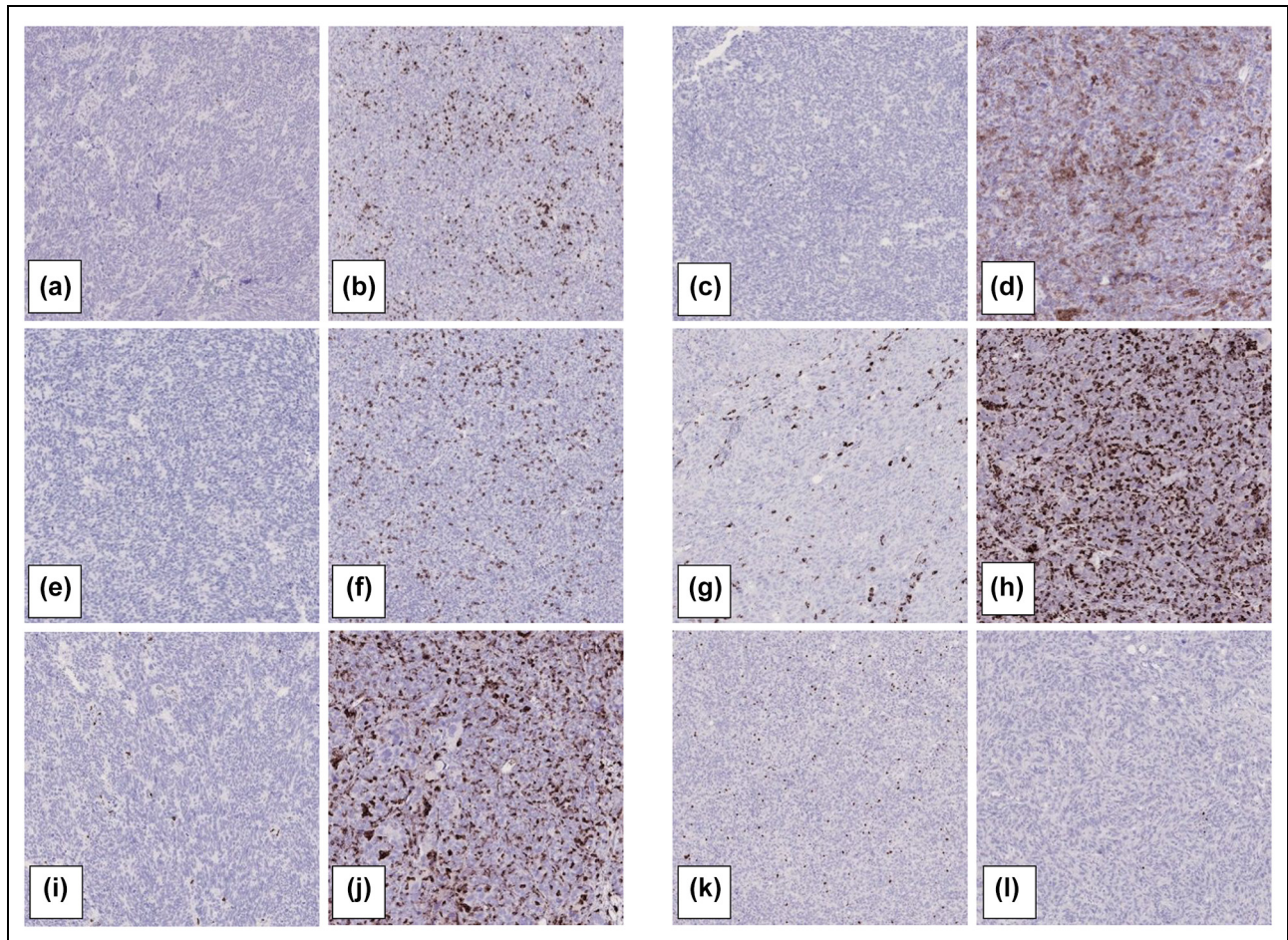
**Figure 1.** Examples of immunostaining patterns.
Granzyme B staining, low (five positive cells/mm^2, (a)) and high (1312 positive cells/mm^2, (b)); CD4 staining, low (four positive cells/mm^2, (c)) and high (1438 positive cells/mm^2, (d)); CD8 staining, low (two positive cells/mm^2, (e)) and high (926 positive cells/mm^2, (f)); CD68 staining, low (positively stained area 4%, (g)) and high (positively stained area 25%, (h)); CD163 staining, low (positively stained area 1%, (i)) and high (positively stained area 20%, (j)); and FoxP3 staining, high (207 positive cells/mm^2, treatment naïve, (k)) and low (seven positive cells/mm^2, NACT treated, (l)).

comparisons) and higher combined CD8+ and granzyme B+ (p = 0.003), granzyme B+ (p = 0.002), CD8+ (p = 0.018) and CD163+ (p = 0.004) cell densities was observed in Kaplan–Meier analysis when the cut-off was set at the 10th percentile (Figure 2). In addition, the higher granzyme B cell density was correlated with PFS when the cut-off was set at first quartile (97 cells/mm^2, PFS 14.00 m vs 17.00 m, p = 0.031). The higher number of granzyme B+ cells was correlated with prolonged median PFS also in univariate Cox proportional hazards regression (HR = 0.820, p = 0.032; Table 5) but only the combined higher amount of both CD8+ and granzyme B+ cells (above 10th percentile) was correlated with prolonged median PFS both in univariate (HR = 0.334, p = 0.006) and multivariate (HR = 0.287, p = 0.002) Cox regression analysis (Table 5). None of the studied immunomarkers was associated with OS (data not shown) or with clinical factors (data not shown).

Table 4. Cell densities (cells/mm^2)^a or positively stained proportions (%)^b/1 mm^2 tumor tissue; median (range).

	Median	Range
FoxP3[a]	99	0–497
Granzyme B[a]	238	3–3028
CD4[a]	180	0–2416
CD8[a]	328	1–4020
CD68[b]	12	2–43
CD163[b]	10	0–35

Post-NACT tumor samples (n = 7) presented with lower densities of FoxP3+ cells (Figure 1(k) and (l); cut-off 10th percentile (9 cells/mm^2), Fisher's exact test, p = 0.013). The median densities of CD4+ and granzyme B+ TILs were more than 50% lower in post-NACT samples, but the differences between groups were not statistically significant (data not shown).
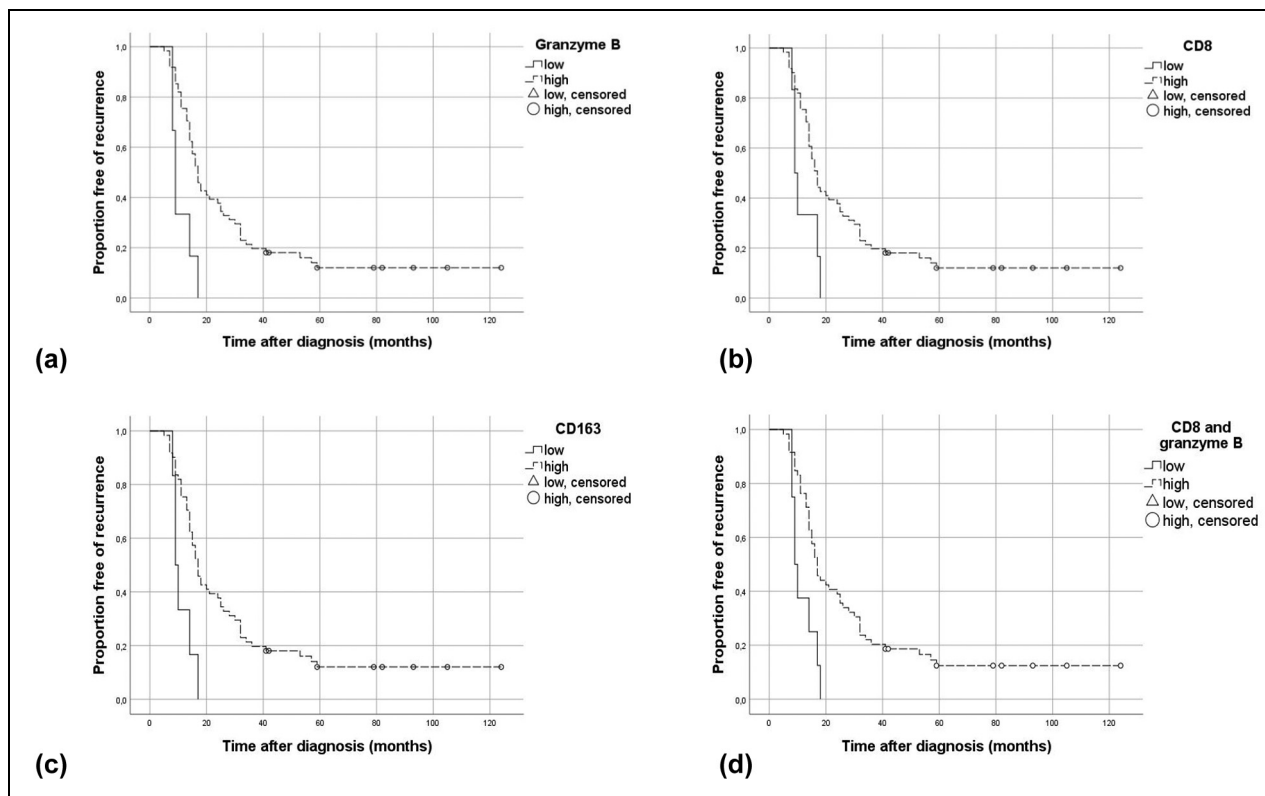
Figure 2. Kaplan–Meier analyses: (a) granzyme B; cut-off 10th percentile (16 cells/mm^2). Log-rank p = 0.002. (b) CD8; cut-off 10th percentile (28 cells/mm^2). Log-rank p = 0.018. (c) CD163; cut-off 10th percentile (3%/mm^2). Log-rank p = 0.004. (d) CD8; cut-off 10th percentile (28 cells/mm^2) and granzyme B: cut-off 10th percentile (16 cells/mm^2). Log-rank p = 0.003.
Numbers of patients at the beginning of follow-up: (a), (b) and (c) low: 6, high: 61 and (d) low: 8, high: 59.

Table 5. Cox proportional hazards regression.

	Univariate			Multivariate		
	Exp (B)	95% CI	p	Exp (B)	95% CI	p
NACT						
No	Reference			Reference		
Yes	2.682	1.447–4.973	0.002	2.275	1.438–5.165	0.002
Optimal cytoreduction						
No (R1/R2)	Reference			Reference		
Yes (R0)	0.409	0.209–0.798	0.009	0.369	0.183–0.744	0.005
Stage						
I/II	Reference			Reference		
III/IV	3.588	1.111–11.590	0.033	2.045	0.606–6.900	0.249
Age	1.002	0.973–1.033	0.886			
FoxP3	0.908	0.748–1.101	0.327			
Granzyme B	0.820	0.684–0.984	0.032			
CD4	0.993	0.855–1.154	0.932			
CD8	0.934	0.794–1.098	0.406			
CD68	0.914	0.550–1.521	0.730			
CD163	0.719	0.475–1.088	0.118			
CD8+ and granzyme B+						
No	Reference			Reference		
Yes	0.334	0.153–0.730	0.006	0.287	0.127–0.648	0.003

Discussion

Here, we report the results of characterization of various TME immunomarkers in a cohort of high-grade serous OC patients. According to our results, combined high intraepithelial CD8 and granzyme B expression correlated with prolonged PFS. Granzyme B is considered as the most important cytolytic enzyme by which activated NK cells and CD8+ TILs destroy tumor cells.[27] The prognostic benefit of CD8+ TILs has been previously shown in many studies.[17–20,22–26] However, the association of CD8+ TILs with improved survival has not been systematically shown in OC throughout all patient subgroups.[25,30] The higher amount of positive, intraepithelial CD8 and granzyme B cells showed statistical significance with longer PFS in multivariate analysis in this study. This might imply that activated NKs and CTLs or other TILs confer the immunogenic phenotype associated with improved survival and that the activation status of CTLs may be as important as the cell density or even more important.[27,30] Previously, Milne et al.[19] found that granzyme B infiltrates were highly correlated with CD8+ TILs while the expression of NK cell markers was low, indicating that granzyme B is mostly expressed by T cells in the TME of HGSC, and therefore, the combined positivity of both CD8 and granzyme B may represent a surrogate marker of activated immune state in the TME. Previously, there has been relatively little data considering the granzyme B expression, or simultaneous expression of CD8 and granzyme B in the TME and OC prognosis, and therefore, the results reported here make a valuable addition to the existing data. It has been shown that higher post-chemotherapy granzyme B+/FoxP3+ cell ratio was associated with better prognosis in HGSC.[30] In addition, a trend toward a positive correlation between granzyme B+ cells and PFS in both post-NACT[30] and treatment naïve[19] OC tumors has been reported.

Here intraepithelial CD4+ or FoxP3+ TILs were not correlated with prognosis. The previous data have been also contradictory with respect to CD4+ TILs and prognosis.[19,22] The previous results concerning the prognostic impact of FoxP3+ T cells are also variable.[18,19,24,28–30] One explanation is that although FoxP3+ TILs are considered immunosuppressive, FoxP3+ TIL density has been found to be highly correlated with other TIL densities, possibly reflecting a strong overall T-cell-mediated immune response.[19] Intraepithelial CD68+ TAM density had no correlation with prognosis in our study. Similarly, various previous studies[19,21,32–34] confirmed no correlation between CD68+ TAMs and OC prognosis. We report here that intraepithelial CD163+ TAMs (M2) were correlated with longer PFS. When analyzing multiple histologic types of OC, CD163+ macrophages have been associated with worse prognosis.[33,34] However, in two studies

with only HGSC patients, controversially, CD163+ TAMs associated with neutral[20] or even favorable[21] prognosis. Although current consensus is that M2 TAMs are immunosuppressive and promote cancer progression,[31] the characterization of macrophages into M1 and M2 types may be excessively simplified.[21]

The results concerning post-NACT samples should be interpreted with caution since the samples are not sequential, and the number of samples was small. However, WSI and DIA methodology confers reliability and the results should not be therefore omitted. We show here that intraepithelial FoxP3+ cell density was significantly smaller in post-NACT samples compared to treatment naïve specimens. The densities of intraepithelial CD4+ and granzyme B+ TILs were considerably smaller in post-NACT samples, as well, but the statistical power was insufficient to show statistical significance. In two separate studies with paired HGSC tumor samples, the density of FoxP3+ TILs remained unchanged after NACT, while an increase in CD8+ and CD3+ TILs,[37] or CD8+, CD4+ and granzyme B+ TILs[30] was observed. In an analysis of unpaired HGSC samples, a decrease in CD3+ sTILs and a trend toward higher ieTIL density post-NACT were observed.[20] Overall, due to methodological differences (paired or unpaired samples, different antibodies and scoring systems, WSI or tumor-array technology with tumor punches, different histological subgroups), the results concerning the effects of chemotherapy on TME have been very diverse and high individual variation between patients has been shown.[20,25,30,36,37] There has been also discussion whether a true comparison between pre- and post-NACT tumors can be performed, since the tumor content or morphology changes tremendously after chemotherapy.[42] However, NACT can alter TME and therefore potentially affect the response to both conventional chemotherapy and immune-oncological therapies. Here, we show changes that can be interpreted as both boosting immunity and silencing it, and therefore, the changes on TME induced by NACT represent an important subject of future studies. Overall, the immune cell counts in post-NACT samples tended to be smaller than in treatment naïve specimens. In addition, NACT and IDS were correlated with shorter PFS and OS when compared to PDS and adjuvant chemotherapy, possibly reflecting to that NACT is administered to patients having an advanced, inoperable disease.

A strength of this study is the homogeneity of the patient cohort: all patients had a high-grade carcinoma. Almost all (96%) patients had HGSC and 90% presented with an advanced stage disease. In various previous studies, multiple histological subtypes have been analyzed. As grade 2 tumors were previously considered as high grade, in some studies with mostly or

exclusively HGSC patients, the patient cohort has consisted with both grade 2 and 3 tumors, enhancing the heterogeneity.

The use of WSI and DIA increased the accuracy and reliability of the results. Using QuPath[40] and ImageJ[41] software, it was possible to scroll the WSI and compare exact cell counts (CD4+, CD8+, FoxP3+ and granzyme B+) and percentages of positively stained areas (CD68+, CD163+) rather than use a semi-quantitative scale for estimating the cell counts or the extent of the staining. The use of DIA has been shown to increase the accuracy of the assessment when compared with the use of a semi-quantitative scale.[38,39] To our knowledge, this report is one of the few studies using WSI and DIA in a cohort of HGSC in assessment of TME content. In addition, methods presented in this study could be applicable for clinical diagnostics.

Our study has also limitations. First, the patient cohort was rather small (n = 67). The number of optimally resected patients was small, as well (n = 16). These features may have affected our results. Previously, a correlation between improved outcome and CD8+[25] or FoxP3+[19] TILs or CD163+ TAMs[21] has been observed only in optimally debulked patients in some studies. Thus, the low R0 rate of this study may have had an impact on the results. The small number of post-NACT samples (n = 7) made the statistical analyses of this group challenging. Paired pre- and post-NACT specimens were not available, and therefore, it was not possible to compare the changes in the immune cell counts pre- and post-NACT on the same patient.

Another limitation is that the archived FFPE samples were analyzed retrospectively. The patients were operated on and the samples collected during a long period of time (2001–2013). Some of the FFPE samples had to be excluded from analysis due to poor quality, which is at least partially due to long period of conservation. The treatment regimen, FIGO staging classification and the criteria for optimal cytoreduction were changed during the period when the patients were treated. During the recruitment period of the study cohort, the breast cancer gene (BRCA)1/2 mutation analysis was not part of the standard of care, and therefore, the BRCA1/2 mutation status was not available in most cases. This should be considered when interpreting the results since the mutation status represents a major prognostic factor in OC. In addition, multiplex IHC stainings on the same specimen were not available, and therefore, it was not possible to study the different immune cell counts or their ratios within the same region of the tumor tissue.

Conclusion

Co-expression of CD8+ and granzyme B+ in TME was correlated with a better prognosis in HGSC, possibly by representing an activated state of immune system and therefore an enhanced anti-tumor immune response in the TME. NACT may affect the immune cell content in the TME and consequently the effect of immuno-oncologic treatments, as well. Further validation studies are needed in larger, prospective OC cohorts for assessment of clinical and especially the predictive significance of combined CD8 and granzyme B positivity as well as the effects of NACT on TME with WSI and DIA.

Author contributions

T.J. has contributed to collecting the clinical data, analyzing the IHC stainings, executing the statistical analyses, and drafting the manuscript; S.L. to planning and supervising the study, scanning and analyzing the IHC stainings, planning and interpreting the statistical analyses, and drafting and revising the manuscript; J.M. to revising and commenting the manuscript, and S.S. to planning and supervising the study, planning and interpreting the statistical analyses, and drafting and revising the manuscript.

Declaration of conflicting interests

The authors declared no potential conflicts of interest with respect to the research, authorship, and/or publication of this article.

Ethical approval

This study has been conducted according to the World Medical Association Declaration of Helsinki and conforms to the ICMJE Recommendations for the Conduct, Reporting, Editing, and Publication of Scholarly Work in Medical Journals. The study protocols have been approved by the Regional Ethics Committee of the Expert Responsibility area of Tampere University Hospital (identification codes: ETL-R09108 and ETL-R11137) for the study. All the study patients have provided a signed informed consent.

ORCID iD

Tiina Jäntti https://orcid.org/0000-0001-6261-5359

Supplemental material

Supplemental material for this article is available online.

References

1. Bray F, Ferlay J, Soerjomataram I, et al. Global cancer statistics 2018: GLOBOCAN estimates of incidence and mortality worldwide for 36 cancers in 185 countries. *CA Cancer J Clin* 2018; 68(6): 394–424.
2. Lheureux S, Gourley C, Vergote I, et al. Epithelial ovarian cancer. *Lancet* 2019; 393(10177): 1240–1253.
3. Reid BM, Permuth JB and Sellers TA. Epidemiology of ovarian cancer: a review. *Cancer Biol Med* 2017; 14(1): 9–32.
4. Berek JS, Kehoe ST, Kumar L, et al. Cancer of the ovary, fallopian tube, and peritoneum. *Int J Gynecol Obstet* 2018; 143(Suppl. 2): 59–178.
5. Perren TJ, Swart AM, Pfisterer J, et al. A phase 3 trial of bevacizumab in ovarian cancer. *New Engl J Med* 2011; 365(26): 2484–2496.
6. Burger RA, Brady MF, Bookman MA, et al. Incorporation of Bevacizumab in the Primary Treatment of Ovarian Cancer. *New Engl J Med* 2011; 365(26): 2473–2483.
7. Vergote I, Tropé C, Amant F, et al. Neoadjuvant chemotherapy or primary surgery in stage IIIC or IV ovarian cancer. *New Engl J Med* 2010; 363(10): 943–953.
8. Kehoe S, Hook J, Nankivell M, et al. Primary chemotherapy versus primary surgery for newly diagnosed advanced ovarian cancer (CHORUS): an open-label, randomised, controlled, non-inferiority trial. *Lancet* 2015; 386(9990): 249–257.
9. Moore K, Colombo N, Scambia G, et al. Maintenance olaparib in patients with newly diagnosed advanced ovarian cancer. *New Engl J Med* 2018; 379(26): 2495–2505.
10. González-Martín A, Pothuri B, Vergote I, et al. Niraparib in patients with newly diagnosed advanced ovarian cancer. *New Engl J Med* 2019; 381(25): 2391–2402.
11. Ray-Coquard I, Pautier P, Pignata S, et al. Olaparib plus bevacizumab as first-line maintenance in ovarian cancer. *New Engl J Med* 2019; 381(25): 2416–2428.
12. Gaillard SL, Secord AA and Monk B. The role of immune checkpoint inhibition in the treatment of ovarian cancer. *Gynecol Oncol Res Pract* 2016; 3: 11.
13. Turner TB, Buchsbaum DJ, Straughn JM Jr, et al. Ovarian cancer and the immune system — the role of targeted therapies. *Gynecol Oncol* 2016; 142(2): 349–356.
14. Drakes ML and Stiff PJ. Regulation of ovarian cancer prognosis by immune cells in the tumor microenvironment. *Cancers* 2018; 10(9): 302.
15. Santoiemma PP and Powell DJ. Tumor infiltrating lymphocytes in ovarian cancer. *Cancer Biol Ther* 2015; 16(6): 807–820.
16. Zhang L, Conejo-Garcia JR, Katsaros D, et al. Intratumoral T cells, recurrence, and survival in epithelial ovarian cancer. *New Engl J Med* 2003; 348(3): 203–213.
17. Hwang W, Adams SF, Tahirovic E, et al. Prognostic significance of tumor-infiltrating T cells in ovarian cancer: a meta-analysis. *Gynecol Oncol* 2012; 124(2): 192–198.
18. Li J, Wang J, Chen R, et al. The prognostic value of tumor-infiltrating T lymphocytes in ovarian cancer. *Oncotarget* 2017; 8(9): 15621–15631.
19. Milne K, Köbel M, Kalloger SE, et al. Systematic analysis of immune infiltrates in high-grade serous ovarian cancer reveals CD20, FoxP3 and TIA-1 as positive prognostic factors. *PLoS ONE* 2009; 4(7): e6412.
20. van Baal JOAM, Lok CAR, Jordanova ES, et al. The effect of the peritoneal tumor microenvironment on invasion of peritoneal metastases of high-grade serous ovarian cancer and the impact of NEOADJUVANT chemotherapy. *Virchows Arch* 2020; 477(4): 535–544.
21. Martin de la Fuente L, Westbom-Fremer S, Skovberg Arildsen N, et al. PD-1/PD-L1 expression and tumor-infiltrating lymphocytes are prognostically favorable in advanced high-grade serous ovarian carcinoma. *Virchows Arch* 2020; 477: 83–91.
22. Pinto MP, Balmaceda C, Bravo ML, et al. Patient inflammatory status and CD4+/CD8+ intraepithelial tumor lymphocyte infiltration are predictors of outcomes in high-grade serous ovarian cancer. *Gynecol Oncol* 2018; 151(1): 10–17.
23. Goode EL, Block MS, Kalli KR, et al. Dose-response relationship of CD8+ tumor infiltrating lymphocytes and survival time in high-grade serous ovarian cancer. *JAMA Oncol* 2017; 3(12): e173290.
24. Hermans C, Anz D, Engel J, et al. Analysis of foxP3+ T-regulatory cells and CD8+T-cells in ovarian carcinoma: location and tumor infiltration patterns are key prognostic markers. *PLoS ONE* 2014; 9(11): e111757.
25. Wouters MCA, Komdeur FL, Workel HH, et al. Treatment regimen, surgical outcome, and t-cell differentiation influence prognostic benefit of tumor-infiltrating lymphocytes in high-grade serous ovarian cancer. *Clin Cancer Res* 2016; 22(3): 714–724.
26. Wang Q, Lou W, Di W, et al. Prognostic value of tumor PD-L1 expression combined with CD8. *Int Immunopharmacol* 2017; 52: 7–14.
27. Rousalova I and Krepela E. Granzyme B-induced apoptosis in cancer cells and its regulation (review). *Int J Oncol* 2010; 37(6): 1361–1378.
28. Zhu Q, Wu X, Wu Y, et al. Interaction between Treg cells and tumor-associated macrophages in the tumor microenvironment of epithelial ovarian cancer. *Oncol Rep* 2016; 36(6): 3472–3478.

29. Shang B, Liu Y, Jiang S, et al. Prognostic value of tumor-infiltrating FoxP3+ regulatory T cells in cancers: a systematic review and meta-analysis. *Sci Rep* 2015; 5: 15179.

30. Pölcher M, Braun M, Friedrichs N, et al. Foxp3+ cell infiltration and granzyme B+/Foxp3+ cell ratio are associated with outcome in neoadjuvant chemotherapy-treated ovarian carcinoma. *Cancer Immunol Immunother* 2010; 59(6): 909–919.

31. Cheng H, Wang Z, Fu L, et al. Macrophage polarization in the development and progression of ovarian cancers: an overview. *Front Oncol* 2019; 9: 421.

32. Ojalvo LS, Thompson ED, Wang T, et al. Tumor-associated macrophages and the tumor immune microenvironment of primary and recurrent epithelial ovarian cancer. *Hum Pathol* 2018; 74: 135–147.

33. Lan C, Huang X, Lin S, et al. Expression of M2-polarized macrophages is associated with poor prognosis for advanced epithelial ovarian cancer. *Technol Cancer Res Treat* 2013; 12(3): 259–267.

34. Yuan X, Zhang J, Li D, et al. Prognostic significance of tumor-associated macrophages in ovarian cancer: a meta-analysis. *Gynecol Oncol* 2017; 147(1): 181–187.

35. Khairallah AS, Genestie C, Auguste A, et al. Impact of neoadjuvant chemotherapy on the immune microenvironment in advanced epithelial ovarian cancer: prognostic and therapeutic implications. *Int J Cancer* 2018; 143(1): 8–15.

36. Mesnage SJL, Auguste A, Genestie C, et al. Neoadjuvant chemotherapy (NACT) increases immune infiltration and programmed death-ligand 1 (PD-L1) expression in epithelial ovarian cancer (EOC). *Ann Oncol* 2017; 28(3): 651–657.

37. Lo CS, Sanii S, Kroeger DR, et al. Neoadjuvant chemotherapy of ovarian cancer results in three patterns of tumor-infiltrating lymphocyte response with distinct implications for immunotherapy. *Clin Cancer Res* 2017; 23(4): 925–934.

38. Pell R, Oien K, Robinson M, et al. The use of digital pathology and image analysis in clinical trials. *J Pathol Clin Res* 2019; 5(2): 81–90.

39. Väyrynen JP, Vornanen JO, Sajanti S, et al. An improved image analysis method for cell counting lends credibility to the prognostic significance of T cells in colorectal cancer. *Virchows Arch* 2012; 460(5): 455–465.

40. Bankhead P, Loughrey MB, Fernández JA, et al. QuPath: open source software for digital pathology image analysis. *Sci Rep* 2017; 7(1): 16878.

41. Schneider CA, Rasband WS and Eliceiri KW. NIH image to ImageJ: 25 years of image analysis. *Nat Methods* 2012; 9(7): 671–675.

42. McCluggage WG, Lyness RW, Atkinson RJ, et al. Morphological effects of chemotherapy on ovarian carcinoma. *J Clin Pathol* 2002; 55(1): 27–31.